Development 139, 335-345 (2012) doi:10.1242/dev.070474
© 2012. Published by The Company of Biologists Ltd

Balancing of ephrin/Eph forward and reverse signaling as the driving force of adaptive topographic mapping

Christoph Gebhardt, Martin Bastmeyer and Franco Weth*

SUMMARY

The retinotectal projection, which topographically maps retinal axons onto the tectum of the midbrain, is an ideal model system with which to investigate the molecular genetics of embryonic brain wiring. Corroborating Sperry's seminal hypothesis, ephrin/Eph counter-gradients on both retina and tectum were found to represent matching chemospecificity markers. Intriguingly, however, it has never been possible to reconstitute topographically appropriate fiber growth in vitro with these cues. Moreover, experimentally derived molecular mechanisms have failed to provide explanations as to why the mapping adapts to grossly diverse targets in some experiments, while displaying strict point-to-point specificity in others. In vitro, ephrin-A/EphA forward, as well as reverse, signaling mediate differential repulsion to retinal fibers, instead of providing topographic guidance. We argue that those responses are indicative of ephrin-A and EphA being members of a guidance system that requires two counteracting cues per axis. Experimentally, we demonstrate by introducing novel double-cue stripe assays that the simultaneous presence of both cues indeed suffices to elicit topographically appropriate guidance. The peculiar mechanism, which uses forward and reverse signaling through a single receptor/ligand combination, entails fiber/fiber interactions. We therefore propose to extend Sperry's model to include ephrin-A/EphA-based fiber/fiber chemospecificity, eventually out-competing fiber/target interactions. By computational simulation, we show that our model is consistent with stripe assay results. More importantly, however, it not only accounts for classical in vivo evidence of point-to-point and adaptive topographic mapping, but also for the map duplication found in retinal EphA knock-in mice. Nonetheless, it is based on a single constraint of topographic growth cone navigation: the balancing of ephrin-A/EphA forward and reverse signaling.

KEY WORDS: Axon guidance, Bidirectional signaling, Ephrin/Eph, Growth cone, Retinotectal, Topographic map, Chick

INTRODUCTION

The computational capabilities of the brain are determined by its connectional architecture, which comprises local circuitry and long-range projections. Projections form the backbone of the neuronal wiring diagram. Their embryonic development is largely genetically instructed, whereas activity is important for later refinement. Molecularly, projection axon guidance has best been investigated for the retinotectal projection, mapping retinal ganglion cell (RGC) axons to the optic tectum (Lemke and Reber, 2005; Luo and Flanagan, 2007; Feldheim and O'Leary, 2010). This map, like numerous others, is topographically organized, i.e. it preserves neighborhood relationships. Thus, RGCs neighboring along the retinal temporal/nasal (t/n) axis project to neighboring positions along the tectal anterior/posterior (a/p) axis. Here, we focus on activity-independent mechanisms of axon guidance along this dimension.

From a wealth of regeneration, in vitro and genetic data, two principles of retinotopic wiring have emerged, which remain difficult to reconcile. Under certain conditions, the wiring displays strict point-to-point specificity (rigid mapping), whereas otherwise it adapts to grossly diverse target fields (adaptive mapping).

Evidence for rigid mapping originates from classical regeneration studies. When the optic nerve is transected and a part of the retina is deleted in adult teleosts or amphibians, the regenerating partial projection selectively targets its original destination, ignoring termination sites vacated by the deletion (Attardi and Sperry, 1963). Recent experiments in the zebrafish indicate that the leading tips of individual RGC axonal arbors map topographically even in the absence of any other retinal fibers (Gosse et al., 2008). This evidence corroborates Roger Sperry's hypothesis (Sperry, 1963), which postulates genetically encoded matching labels on fiber terminals and target sites [fiber/target (FT) chemospecificity]. Indeed, tectal cell membranes convey graded repulsive signals (a<p) to retinal fibers in vitro (Bonhoeffer and Huf, 1982) owing to the expression of ephrin-As sensed through counter-graded retinal EphA receptors (Cheng et al., 1995; Drescher et al., 1995). Eventually, individual ephrin-A/EphA expression patterns were found to sum up to counter-gradients along both the retinal n/t and the tectal a/p axis (Fig. 1A). Ephrin-A/EphA forward, as well as reverse, signaling exert repulsive actions on RGC growth cones in vitro (Monschau et al., 1997; Rashid et al., 2005) and genetic deletions in mice suggest corresponding roles in vivo (Feldheim et al., 2000; Feldheim et al., 2004). Surprisingly, however, it has never been possible to reconstitute fully topographically appropriate growth of RGC fibers in vitro using the identified guidance molecules. Thus, in choice assays (Walter et al., 1987; Vielmetter et al., 1990), in which retinal fibers are confronted with alternating stripes of ephrin-A and a neutral substrate (here called single-cue stripe assay), nasals never decide properly. The reasons for this failure have remained puzzling.

The concept of rigid chemospecificity was first challenged by other seminal regeneration experiments, which instead promoted the concept of adaptive mapping (reviewed by Goodhill and Richards, 1999). When a regenerating half-retina innervates a full tectum, terminals only initially occupy their proper tectal half.

Zoological Institute, Department of Cell- and Neurobiology, Karlsruhe Institute of Technology (KIT), D-76131 Karlsruhe, Germany.

*Author for correspondence (franco.weth@kit.edu)

Accepted 3 November 2011

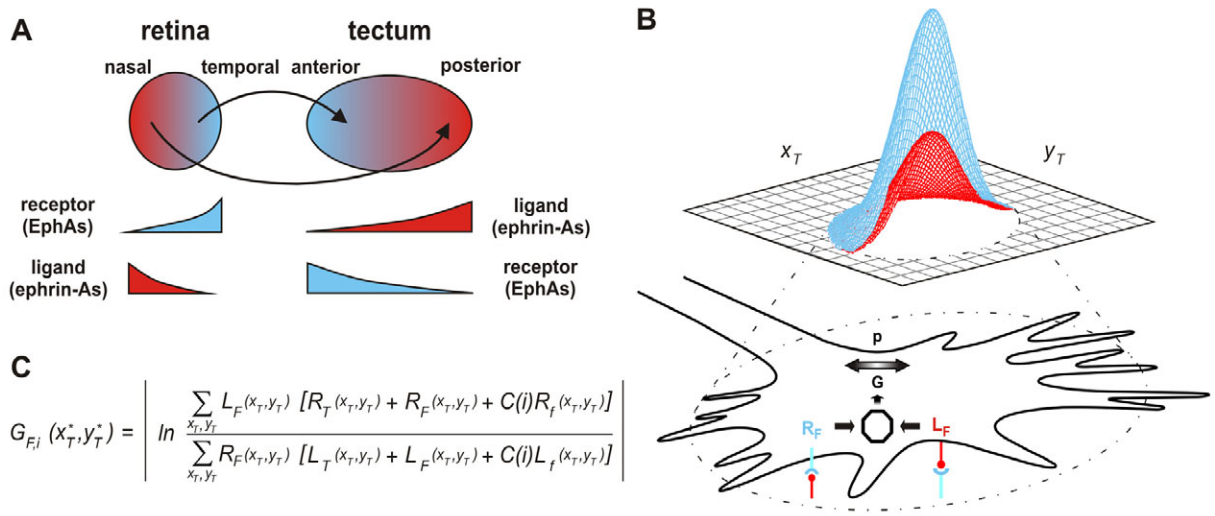

Fig. 1. A single-constraint model of topographic axonal mapping. (**A**) Temporal and nasal fibers terminate in the anterior and posterior tectum, respectively. Exponential gradients represent cumulative distributions of ephrin-A ligands (red) and EphA receptors (blue) in retina and tectum. (**B**) A fiber terminal is modeled by a circular disc with center position (x^*_T,y^*_T), endowed with bell-shaped receptor (blue) and ligand (red) profiles, according to its topographic origin. Guidance cues are detected via receptor, R_F, and ligand, L_F. Resulting forward and reverse signals are integrated to yield the guidance potential, G, which is used to determine the probability p to change position. (**C**) The guidance potential $G_{Fi}(x^*_T,y^*_T)$ of fiber F in iteration i. L_FR_T, R_FL_T: reverse and forward fiber-target interactions. L_FR_F, R_FL_F: cis-interactions. $C(i)L_FR_f$, $C(i)R_FL_f$: weighted fiber-fiber interactions. The topographic target is reached when $G_{Fi}=0$, i.e. when reverse and forward signaling are balanced.

After longer regeneration periods, the projection spreads to cover the whole target evenly (expansion) (Schmidt et al., 1978). Conversely, the projection of a full retina properly scales to a half-tectum (compression) (Gaze and Sharma, 1970). When a nasal half-retina is forced to innervate an emptied anterior half-tectum (mismatch), a normally oriented half-map develops on the foreign field (Horder, 1971). If in a similar experiment the occupied p-tectum is left in place when the a-tectum is de-afferentiated, a second nasal population again forms a half-map on the foreign anterior target, but now with reversed orientation (polarity reversal) (Meyer, 1979). These results have usually been taken to indicate guidance mechanisms based on fiber/fiber (FF) interactions, the molecular underpinnings of which, however, are unknown. Recently, FF interactions have gained renewed interest. When, in a scattered half-population of RGCs, a constant amount of EphA is added by transgenic expression, a map duplication occurs, in which knock-in terminals occupying the a-tectum displace wild-type terminals posteriorly (Brown et al., 2000; Reber et al., 2004).

These seemingly conflicting bodies of evidence have been accompanied by numerous attempts at computational modeling (reviewed by Goodhill and Xu, 2005; van Ooyen, 2011). Although many models addressed certain aspects, at least four were successful in conceptually reconciling rigid and adaptive mapping evidences (Fraser and Perkel, 1990; Weber et al., 1997; Willshaw, 2006; Simpson and Goodhill, 2011). Neither of them, however, rigorously relies on experimentally observed ephrin-A/EphA-based guidance mechanisms. Significantly, none of them has successfully addressed the seminal results of stripe assay experiments.

Here, by introducing novel receptor/ligand (‘double-cue’) stripe assays, fabricated by a combination of microfluidic network and contact-printing techniques, we demonstrate the possibility to reconstitute topographically appropriate guidance of RGC growth cones in vitro, revealing that the simultaneous presence of forward and reverse FT signaling is sufficient for rigid topographic growth decisions. To additionally cover adaptive mapping, we suggest extending Sperry’s model to include FF chemospecificity, also based on ephrin-A/EphA bidirectional signaling. We present a comprehensive model for the guidance of topographically projecting axons that is essentially based on the single constraint of balancing ephrin-A/EphA forward and reverse signaling. In computational simulations, it successfully replicates evidences for both, rigid and adaptive mapping.

MATERIALS AND METHODS

Simulations

All simulations were run using MATLAB 7.8 (MathWorks, Natick, MA, USA). The target field was an (X_T-by-Y_T) rectangular array of unit-sized square increments, (x_T,y_T). Each increment displayed a combination of target-borne ligand and receptor concentrations [$L_T(x_T,y_T)$, $R_T(x_T,y_T)$], amounting globally to stripes of constant values in the x_T direction or to reciprocal exponential gradients [$L_T(x_T,y_T)=\exp(\gamma(x_T-\delta/2))$, $R_T(x_T,y_T)=\exp(-\gamma(x_T-\delta/2))$; defaults: gradient decay constant $\gamma=0.05$, gradient extent $\delta=50$; anterior: $x_T=1$].

A retinal n/t strip was represented by a field of (50×1) unit squares. A retinal fiber terminal specified by its topographic assignment (x_F) in this field was attributed reciprocal values of axonal receptor, $R_F(x_F)$, and ligand, $L_F(x_F)$ [$R_F(x_F)=\exp(\alpha(x_F-\beta/2))$, $L_F(x_F)=\exp(-\alpha(x_F-\beta/2))$, default $\alpha=0.05$, $\beta=50$; nasal: $x_F=1$]. x_F values for n terminals are n evenly spaced numbers from the continuous interval [0,β] rounded to the nearest integer.

The receptor/ligand profile of an individual terminal centered at (x^*_T,y^*_T) was modeled by a two-dimensional Gaussian function $F(x_T,y_T)=\exp(-(a(x_T-x^*_T)\text{^}2+b(y_T-y^*_T)\text{^}2))$, with a=b=0.5. All values $F(x_T,y_T)<0.01$ were set zero, resulting in $F_{0.01}(x_T,y_T)$, representing a bell-shaped function with a diameter of about 7 units surrounded by zero entries. $F_{0.01}(x_T,y_T)$ was multiplied by $R_F(x_F)$ or $L_F(x_F)$, according to the topographic origin of the fiber, yielding terminals with radially decreasing $R_F(x_T,y_t)$ and $L_F(x_T,y_t)$ values. Matrices of cumulative fiber-borne guidance cues $R_f(x_T,y_T)$ and $L_f(x_T,y_T)$, which represent the current global distribution of these cues, were calculated in each iteration by summing for each square of the field the respective contributions of all individual terminals, except the one under consideration.

The guidance potential at each unit square comprises forward (FWD) and reverse (REV) signaling, each consisting of FT, cis- and FF interactions. Individual terms were calculated from mass action, according to REV=$k_{-1}KL_FR$ and FWD=k_1KR_FL, with k_1, k_{-1} and K being proportionality and binding constants. k_1 and k_{-1} are set equal for reasons of simplicity. The potential detected by the complete fiber terminal F at position (x^*_T,y^*_T) in iteration i, $G_{F,i}(x^*_T,y^*_T)$, is calculated from mean reverse and forward signals, each of which is averaged over all the fields underlying the terminal (Fig. 1C). To reflect conceptually the increases in terminal number and size, trans FF interactions were weighted by a dynamic factor, C(i), which ramps up with iteration number, while actual simulations run with the full complement of fixed-size terminals from the outset. C(i) is calculated by the saturating sigmoid function C(i)=C_0(–exp(–ln(2^((i/j)^s)))+1), with C_0 being the maximum value, j the iteration number of half-maximal value for C(i) and s determining steepness. Absolute value and logarithm were used for calculating $G_{F,i}$ to simplify integration into the probabilistic movement algorithm (see below). $G_{F,i}$ is not defined for L_F, R_F=0. This could be avoided by additive constants representing baseline forward/reverse signaling, which we omitted for simplicity.

At iteration i=1, fiber terminals were placed either in random or in topographic order along the y_T-axis (x_T=1) of the target field. Fiber terminal movement instructed by $G_{F,i}$ was adopted from the servo-mechanism model (Honda, 1998). During each iteration, a terminal randomly chooses one of the (3×3) squares centered on its current position, (x^*_T,y^*_T), for evaluation. Should a terminal choose a positional coordinate outside the target field, the respective coordinate is reset to the current value. Choosing an occupied square was permitted, i.e. no competition for target space was implemented. Eventually, the terminal determined the potential $G_{F,i}$ at the current position, (x^*_T,y^*_T), and $G'_{F,i}$ at the chosen position, $(x^{*\prime}_T,y^{*\prime}_T)$. For a probabilistic step decision, the values pd($G_{F,i}$) and pd($G'_{F,i}$) were calculated from a Gaussian distribution pd($G_{F,i}$)=(1/(σ√(2π)))exp(–$G_{F,i}$^2/(2σ^2)) with standard deviation σ. The probability, p, of changing the position is given by p=pd($G'_{F,i}$)/(pd($G_{F,i}$)+pd($G'_{F,i}$)). Unless explicitly stated, a unique set of parameters was used in all simulations (number of terminals *n*=200; (50×8) target field; 30,000 iterations; FF interaction parameters: C_0=100, j=15,000, s=5; σ=0.12).

For comparative purposes, we used an alternative model (Honda, 1998). Instead of balancing two counteracting monofunctional cues (G=|ln(REV/FWD)|), Honda's model uses one cue that is rendered bifunctional by calculating deviations from a deliberate set-point constant, S (G=|S-FWD|). The constant was set to S=0.2143 (mean of the non-zero entries of $F_{0.01}$, see above) and σ was set to σ=0.07 to accommodate our remaining parameters.

Stripe assays

Single-cue stripe assays were performed as described previously (Hornberger et al., 1999; von Philipsborn et al., 2006; von Philipsborn et al., 2007). For EphA3 assays a solution of 30 μg/ml EphA3-Fc fusion protein (R&D Systems, Minneapolis, MN, USA) containing 2 μg/ml Alexa594-labeled anti-human-Fc antibody (Invitrogen, Carlsbad, CA, USA) was adsorbed from the microfluidic channels (90 μm) of a custom-made silicon matrix to the surface of a Petri dish (3 hours at 37°C). For contact printing of ephrin-A2, 16 μg/ml purified ephrin-A2-Fc (R&D Systems) was pre-clustered with 48 μg/ml Alexa594-labeled anti-human-Fc antibody for 30 minutes at 25°C. Afterwards, the matrix channel field was coated with the protein solution for 30 minutes at 37°C, washed with distilled H_2O and dried with N_2. It was then stamped onto a Petri dish for 3 hours at 37°C. Substrates were overlaid with 20 μg/ml laminin (Invitrogen) for 1 hour and eventually covered with F12 medium. Ephrin-A2/EphA3 double-cue substrates were fabricated by printing ephrin-A2 into the Petri dish, but with the matrix remaining in place. Subsequently, EphA3 was absorbed from solution injected into the channels, generating separated alternate stripes of both proteins.

Explant cultures

Retinae of E6-E7 chick embryos were dissected in ice-cold Hanks' medium, placed on nitrocellulose filters and cut into 250 μm wide n/t-strips. Explants were placed on the stripe substrates and grown in F12 medium containing 0.4% methylcellulose, 2% chicken and 5% fetal calf serum. After 20-24 hours, the cultures were fixed and stained with Alexa-488-phalloidin (Invitrogen).

RESULTS

A novel model of chemospecificity-driven topographic mapping

To model the dynamics of chemospecifically interacting projection axon terminals on targets carrying chemospecificity cues, we used a grid composed of unit-sized squares as the target field. Each square increment displayed a predefined concentration of target-borne EphA receptors (R_T) and ephrin-A ligands (L_T), respectively, amounting to gradients or stripe patterns across the field. In our model, fiber terminals are assumed to represent growth cones during early development and terminal arborizations later on. Accordingly, their movement corresponds to active migration (growth cones) or to shifting by extension/retraction of protrusions (terminal arbors). Fiber terminals are collectively modeled as approximately circular discs, about 7 units in diameter. They carry surface concentrations of fiber-borne ephrin-A (L_F) and EphA (R_F). As only thin protrusions (filopodia or branchlets) radiate from a real terminal, its interaction efficiency will fade with radial distance. Correspondingly, we modulate surface concentrations of R_F and L_F on the fiber terminal by a two-dimensional bell-shaped function centered on the terminal's midpoint and truncated at its perimeter (Fig. 1B). The ratio of both concentrations, which is constant across the terminal, encodes topographic origin.

In every iterative step of a simulation, each terminal compares its current position to a randomly chosen adjacent position and decides, according to the model's guidance criterion, whether to take the new position. Terminals can freely overlap at all stages of the simulation.

To derive the guidance criterion, we conceive axon targeting as the search for the minimum of a potential arising from the action of guidance cues (Gierer, 1981). In principle, the minimum could either be due to the bifunctional action of one cue (e.g. attraction below and repulsion above a threshold concentration signifying the target) or to the monofunctional actions of two counter-current cues. In single-cue stripe assays, both EphA7-mediated reverse and ephrin-A5-mediated forward signaling solely convey repulsive signals to chick RGC growth cones (Drescher et al., 1995; Rashid et al., 2005). Responsivity decreases with cue concentration, but it has never been observed to switch to attraction. Therefore, we tentatively assume monofunctional actions. In our model, like in vivo, ephrin-A ligands and EphA receptors follow counter-graded distributions in retina and tectum (Fig. 1A). To implement monofunctional actions, we assume reverse (REV) and forward (FWD) signals to be simply proportional to the concentration profiles of their respective cue (mass action). Thus, though varying with cue concentration the signal always stays repulsive and never switches to attraction. Inspired by the treatment of activators and inhibitors in enzyme kinetics, we use the ratio of the two signals, REV/FWD, to determine the guidance potential. To simplify algorithmic processing, we use the absolute value of the logarithm of this ratio to calculate numerically the guidance potential, G (Fig. 1C). Whenever reverse and forward signaling get out of balance (REV/FWD≠1) the terminal experiences an unfavorable positive potential. Every attempted movement causing a potential decrease is favored and the target is reached when the potential is zero, i.e. when REV/FWD=1.

The most intuitive means to conceivably construct a potential minimum from monofunctional cues would be two independent repulsive ligands arranged countercurrently across the target and

sensed by two independent receptors on every terminal. Here, however, one signal is the reverse of the other, resulting in the simultaneous presence of receptor and cognate ligand on the terminals. This entails FF interactions in cis and trans that would otherwise not occur. Thus, REV and FWD are each composed of three additive components of ephrin-A/EphA signaling. First, reverse and forward FT interactions represent Sperry-type chemospecificity. Second, cis-interactions on each terminal have to be considered, e.g. between colliding filopodia of the same growth cone. We treat these interactions equivalently to trans-interaction in terms of their signal transduction. Third, the simultaneous presence of ligands and receptors on all terminals also inevitably causes FF interactions in trans. Their impact will be small initially, when the first growth cones enter the target. Later, however, as more fibers arrive and develop terminal arborizations, FF interactions will become more frequent and eventually dominate FT interactions.

As FT, cis- and FF interactions remain indistinguishable to the terminal, our model amounts to a single guidance constraint: the balancing of reverse and forward ephrin-A/EphA signaling. For full mathematical detail, see Materials and methods.

Testing the basic performance of the model

A test fiber terminal, exploring a field devoid of target cues but containing two other terminals (Fig. 2A), experiences no guidance potential (Fig. 2A′) in the absence of overlap. In this case, only reverse and forward cis-signals are impinging, which are inherently balanced. Once overlapping, a repulsive potential arises that is proportional to the degree of overlap with the maximum, depending on the topographic disparity of the interacting terminals. Identical twin terminals will not elicit any potential because their interaction does not imbalance forward and reverse signaling. Accordingly, a test terminal probing an array of topographically ordered terminals (Fig. 2B) will detect a sharp minimum of the total potential at its topographically appropriate place in the array (Fig. 2B′). These features underlie the self-sorting capabilities of the terminals in our model, which are needed in instances of adaptive mapping once target-derived cues have been superseded. A similar but much more shallow potential arises in a field containing target-borne guidance cues only (Fig. 2C,C′). The minimum now indicates the topographically correct position on the target field. Finally, the potential on a field containing both target-derived cues and a dense population of ordered terminals (Fig. 2D,D′) resembles the potential due to FF interactions, because FF chemospecificity dominates FT chemospecificity in proportion to C(i) in Fig. 1C.

Robust topographic mapping

Topographic mapping is indicated throughout this study by fiber terminal positions lying on the main diagonal of a mapping plot, in which the final coordinate on the target a/p axis is depicted as a function of topographic origin on the retinal n/t axis. All simulations ran to convergence (30,000 iterations), indicated by G values around zero and the absence of any net terminal movement. With matching counter-gradient systems on retina and tectum (Fig. 3A), targeting precision decreases with decreasing gradient steepness, but topographic order per se is robust towards alterations of the gradient shape. The same even holds true if retinal and tectal gradient systems do not match (Fig. 3B, dots). Decreased targeting precision in altered gradients might underlie the formation of ectopic termination zones found in ligand/receptor deletion mutants. Condensation into focused termination zones, however, needs correlated activity (McLaughlin et al., 2003), which is not incorporated in our model. Without FF chemospecificity, corresponding mismatches cause severe mistargeting (Fig. 3B, crosses).

Topographically differential repulsion

There has been a long-standing debate as to whether tectal ephrin-As might suffice to guide axons topographically, i.e. if they acted in a bifunctional manner (Gierer, 1981; Honda, 1998; Hansen et al.,

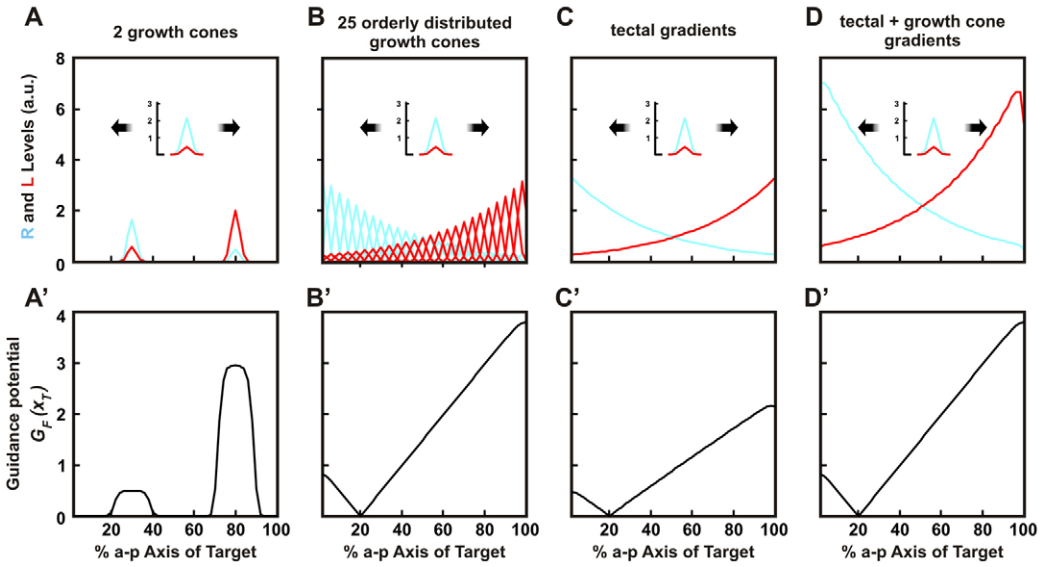

Fig. 2. Basic performance of the model. (**A**,**A′**) A fiber terminal originating from x_F=10 (20% temporal) in the retina is probing via its receptor (blue) and ligand (red) a 50×1 target field containing nothing but two randomly placed terminals (x_F=15 and x_F=40). Non-zero potentials due to terminal overlap are causing repulsion, which is the smaller the more topographically similar the interacting terminals. (**B**,**B′**) In a field containing nothing but 25 topographically ordered terminals, the probing terminal detects G_F=0 at the correct target. (**C**,**C′**) Topographic mapping by target-derived guidance cue gradients without other terminals, as indicated by G_F=0 at the correct target position. (**D**,**D′**) The total potential calculated from FF and FT interactions preserves its minimum at the correct topographic position.

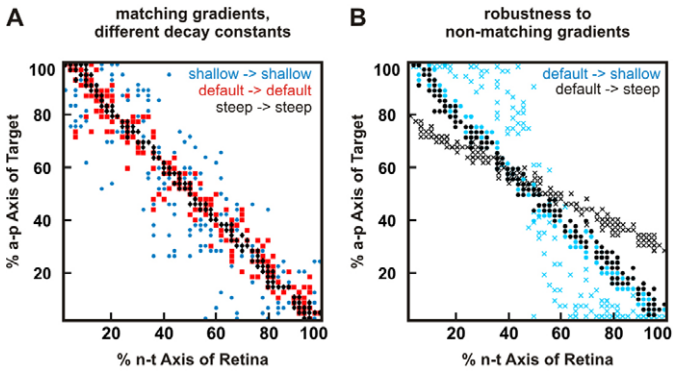

Fig. 3. Topographic and robust mapping. (**A**) Mapping plot of the final positions of 200 randomly seeded fibers along the a/p axis as function of n/t origin. Topography is preserved but precision decreases with decreasing steepness of matching gradients (decay constants for steep, default and shallow gradients $\alpha=\gamma=0.1$, 0.05 and 0.01, respectively). (**B**) Non-matching gradients in retina and target. Mapping is robust (blue and black dots) when FF interactions are active ($C_0=100$). Otherwise ($C_0=0$), distorted maps are formed (blue, black crosses) (decay constants $\alpha=0.05$, $\gamma=0.1$ and 0.01).

2004). Alternatively, they could act monofunctionally and need a counteracting tectal cue to achieve topographic guidance. To address this issue, we compared single-cue stripe assays simulated with our model (monofunctional) and an alternative one based on bifunctional ephrin-A action (Honda, 1998) with experimental results.

At high cue concentrations, simulations with both models concordantly predict topographically non-differential avoidance of stripes containing either ligand or receptor (Fig. 4A,A′,C). At lower concentrations, however, predictions diverge. In our model, simulated trajectories become topographically differential. In simulations of ligand stripe assays (Fig. 4A″), for example, nasal fibers become indiscriminative, whereas temporals continue to avoid the cue. Notably, albeit topographically differential this is not topographically appropriate, because nasals, instead of becoming indiscriminative, should use high ephrin-A concentrations as their cognate mapping cue, according to tectal expression patterns. The bifunctional model, by contrast, yields a markedly different result. At low concentrations, it predicts topographically appropriate behavior, with temporals deciding against and nasals for the ligand stripes (Fig. 4C″). Experimentally, we find robust uniform repulsion in single-cue stripe assays using high concentrations of ephrin-A2 (16 μg/ml) or EphA3 (30 μg/ml; Fig. 4B,B′). At reduced concentrations (8 μg/ml ephrin-A2 in Fig. 4B″), the decision becomes topographically differential. At neither concentration of ligand or receptor do we achieve topographically appropriate behavior in accordance with our model. Thus, although our tentative assumption of monofunctionally acting guidance cues is immediately consistent with the experimental data, bifunctionality is not, although it cannot conclusively be ruled out based on this negative evidence.

The effect of cis-interactions

To revisit cis-interactions, we simulated the stripe-assay experiments that had first revealed their existence (Hornberger et al., 1999). When, in ligand stripe assays normally showing a topographically differential result (moderate ephrin-A2 concentration), axonal ephrin-A is shed, growth cone behavior switches to uniform repulsion. Conversely, when the axonal ligand is overexpressed, uniform desensitization is observed. This is exactly what we find in our simulations (Fig. 5). As similar effects can also be demonstrated in single axon simulations (supplementary material Fig. S1), they do not depend on trans FF interactions. Remarkably, our model does not implement any masking or attenuating effect of cis-interactions, which were previously suggested. Instead, cis-interactions in our model simultaneously release equal amounts of reverse and forward signals into the same terminal, which contribute to the total balance of signals without eliciting any overt response of the terminal. In low-concentration ligand stripe assays, signaling in nasal growth cones is dominated by cis-interactions and, thus, is nearly balanced on either stripe. When the axonal ligand is shed, this dominance is lost and the de-balancing (repulsive) action of the ligand stripe is unveiled. By contrast, signaling in temporal growth cones on ligand stripes is dominated by forward FT interactions and is therefore strongly out of balance, resulting in avoidance. When the axonal ligand is overexpressed, cis-signaling prevails and thereby introduces its balancing effect, prompting growth cones to ignore the cue.

Topographically appropriate guidance in vitro

The fact that, in single-cue stripe assays, neither ephrin-A nor EphA elicits topographically appropriate guidance in RGC growth cones has remained a major challenge to the notion that those cues were sufficient for topographic mapping. Given that both appear to act monofunctionally, we supposed that a guidance potential permitting appropriate decisions could be constituted by combining them. Therefore, we first simulated a novel type of stripe assay with alternating stripes of receptor and ligand (double-cue stripe assay). In fact, these simulations predicted topographically appropriate substrate choice, with n-axons on ligand and t-axons on receptor stripes (Fig. 6A).

To test this prediction experimentally, substrates with alternating receptor and ligand stripes were fabricated. The method routinely applied for stripe carpet fabrication is unsuitable here owing to the high affinity of ephrin-A/EphA binding, which results in mutual masking of the proteins co-deposited on the culture dish. Therefore, a novel substrate patterning technique, which relies on simultaneous protein contact-printing and physisorption from microfluidic channels of the printing stamp, was established (see Materials and methods).

Notably, at concentrations of 30 μg/ml EphA3 versus 16 μg/ml ephrin-A2, topographically appropriate fiber growth was observed. Nasal axons grew on ephrin-A2 stripes, whereas t-axons of the same explant grew on EphA3 (Fig. 6B). Central fibers did not show any decision, probably indicating a continuous position-dependent transition of guidance behavior. A wide range of EphA3/ephrin-A2 concentration ratios had to be tested experimentally to obtain this result. At higher ratios, the results reproducibly resembled EphA3 single-cue stripe assays (‘reverse-like’; Fig. 6C, upper row); at lower ratios they resembled ephrin-A2 single-cue stripe assays (‘forward-like’; Fig. 6C, lower row). This agrees with our computational simulations, which predict that the outcome is likely to be critically sensitive to the ratio of ligand/receptor concentrations in the stripes (supplementary material Fig. S2). If both proteins are not applied with balanced surface activity, all axons will grow either on the receptor or on the ligand stripes, depending on whose activity is in excess. On substrates made of 30 μg/ml EphA3 versus 16 μg/ml ephrin-A2, a proper topographic response occurred in 19.5% of the analyzed

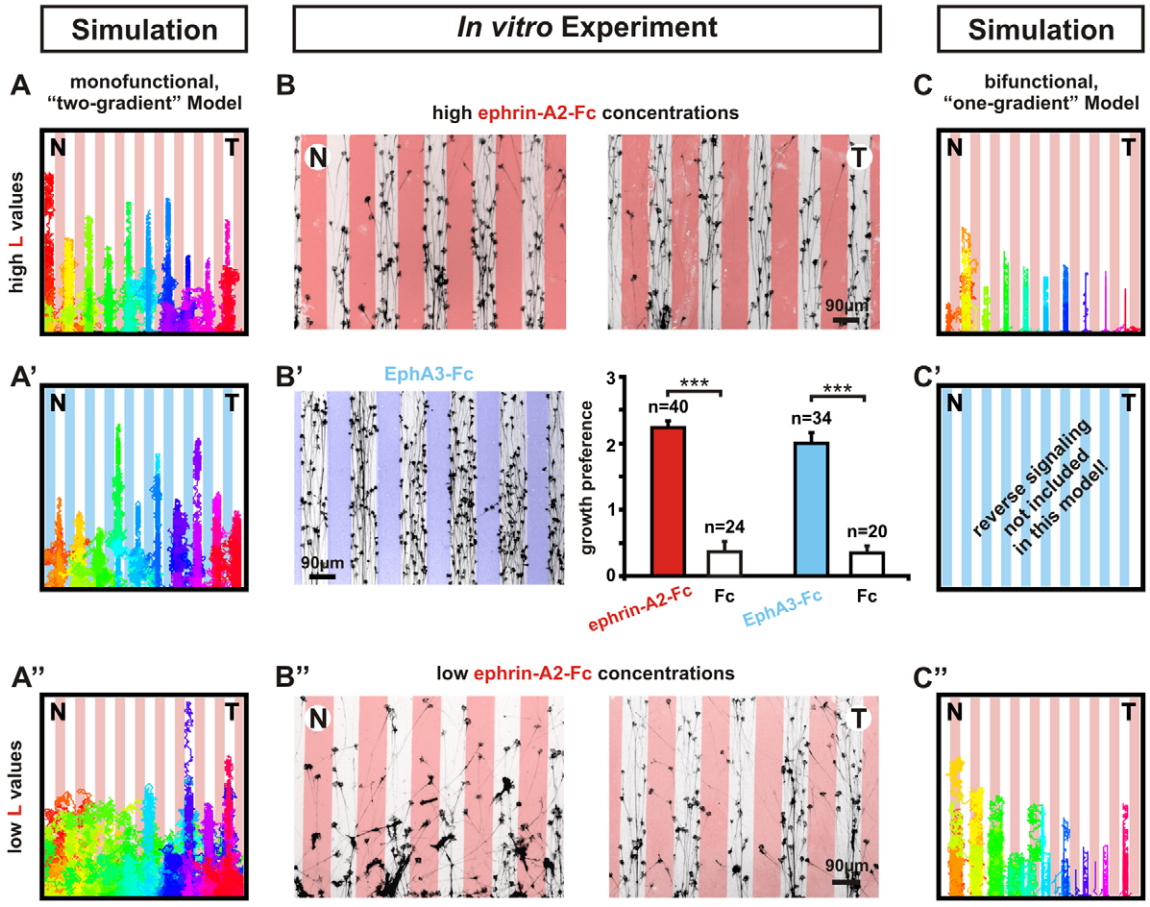

Fig. 4. Single-cue stripe assays suggest monofunctional action of guidance cues. Stripe assays simulated with the present monofunctional versus a bifunctional guidance model compared with experimental results. Fiber trajectories are depicted in rainbow colors for discrimination [n=50, 3000 iterations, 100×100 field, 20 stripes, each 5×100]. (**A-A″**) In our model, all fibers non-differentially avoid (A) high ligand (red: L_{T2}=1, R_{T2}=0; white: L_{T1}=0, R_{T1}=0) or (A′) high receptor (blue: L_{T1}=0, R_{T1}=1; white: L_{T2}=0, R_{T2}=0). (A″) A topographically differential, but not appropriate, decision is seen at low ligand values (red: L_{T2}=0.2, R_{T2}=0; white: L_{T1}=0, R_{T1}=0). (**B**,**B′**) Experimental in vitro stripe assays showing nasal and temporal fibers avoiding 16 μg/ml ephrin-A2-Fc (red) and 30 μg/ml EphA3-Fc stripes (blue). Quantification according to the scoring system of Walter et al. (Walter et al., 1987), with zero indicating no decision and 3 indicating very strong decision (P<0.001, Student's t-test, error bars represent s.e.m.). (**B″**) Stripe assays using low concentrations of ephrin-A2 (8 μg/ml) show a topographically differential, but not appropriate, decision. (**C**) With a bifunctional model based on forward signaling, all fibers avoid high ligand values (red: L_{T2}=1; white: L_{T1}=0). (**C′**) Reverse signaling is not defined in a bifunctional model relying on one cue only. (**C″**) With low ligand values (red: L_{T2}=1.8; white: L_{T1}=0) a never observed topographically appropriate decision is predicted, with nasals preferring and temporals avoiding the ligand. Experimental evidence is consistent with monofunctional, but not with bifunctional action of the guidance cues.

explants (Fig. 6C, middle row). Although using the same nominal concentrations, the remaining cases were reminiscent of stripe assays in which one of the cues was in excess ('forward- or reverse-like'). This instability is most probably caused by inevitable micro-inhomogeneities of the printed ephrin-A2 stripes, causing local concentration fluctuations that disturb the delicate equilibrium (supplementary material Fig. S3). Importantly, however, no explant was found in which n-axons grew on EphA3 and temporals on ephrin-A2 concomitantly ('anti-topographic behavior').

Modeling in vivo evidence for rigid and adaptive topographic mapping

In the zebrafish, the distal tips of single RGC arbors are able to map properly in the absence of any other retinal fibers (Gosse et al., 2008). Correspondingly, we performed 300 simulations of single, randomly selected retinal terminals migrating on the target field in isolation. Their stable final positions were accumulated in a mapping plot, indicating proper topographic mapping (Fig. 7A). This is, because our model mostly relies on Sperry-type FT interactions, as long as the target is only sparsely populated.

Recent seminal genetic evidence for the importance of FF interactions come from EphA3 knock-in mice (Brown et al., 2000). We simulated the corresponding experiments with 200 terminals (Fig. 7B), assigning to every other an additional amount of axonal receptor (red, knock-in; blue, wild type). Simulations of homozygous (ki/ki) and heterozygous (ki/+) maps showed the experimentally observed duplications, with the separation being more severe in homozygotes. However, a mapping collapse among temporals, which has been reported for the heterozygotes, was not observed. Recent modeling approaches suggest that this collapse is due to a competition of chemospecificity-driven and Hebbian activity-dependent mechanisms (Tsigankov and Koulakov, 2010),

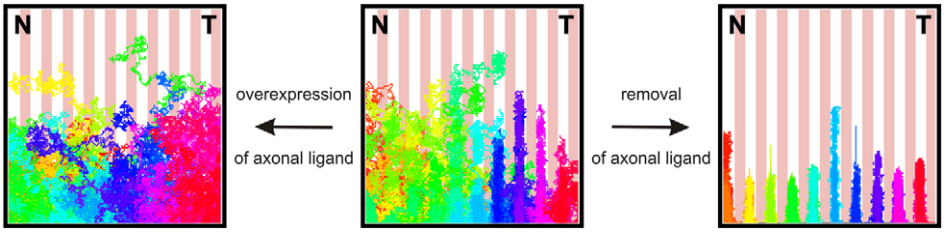

Fig. 5. Modeling the effect of axonal cis-interactions. Based on low ligand stripe assays (middle; red: L_{T2}=0.2, R_{T2}=0; white; L_{T1}=0, R_{T1}=0), assigning a uniform amount of L_F to all fibers (left; L_F=5, 'overexpression') leads to a loss of sensitivity. Reduction of L_F (right; L_F=0.01) leads to uniform avoidance. This agrees with experimental findings (Hornberger et al., 1999), although no masking/signal attenuation is implemented in the present model [*n*=50, 3000 iterations, 100×100 field].

the latter of which we do not address. Without FF interactions, our model is in conflict with the experimental results: homozygous knock-in terminals do not invade the target and wild-type terminals remain unaffected (Fig. 7B, gray crosses).

Classical regeneration experiments first indicated the importance of FF interactions. We simulated expansion experiments (Schmidt et al., 1978) with 100 terminals randomly taken from either the nasal or temporal half-retina migrating on a denervated full-sized tectum. After 5000 iterations, nasal as well as temporal projections covered their respective tectal halves. However, after 30,000 iterations, both projections had expanded and formed a stable topographic map covering the whole field (Fig. 7C) as in the corresponding experiments. In vivo, expansion is thought to occur only when fibers of the previous innervation have disappeared. Correspondingly, when we run the same simulation on top of a complete retinal projection, representing remnants of the previous innervation, no expansion occurs even after 30,000 iterations ('pre-occupied tectum', Fig. 7C′).

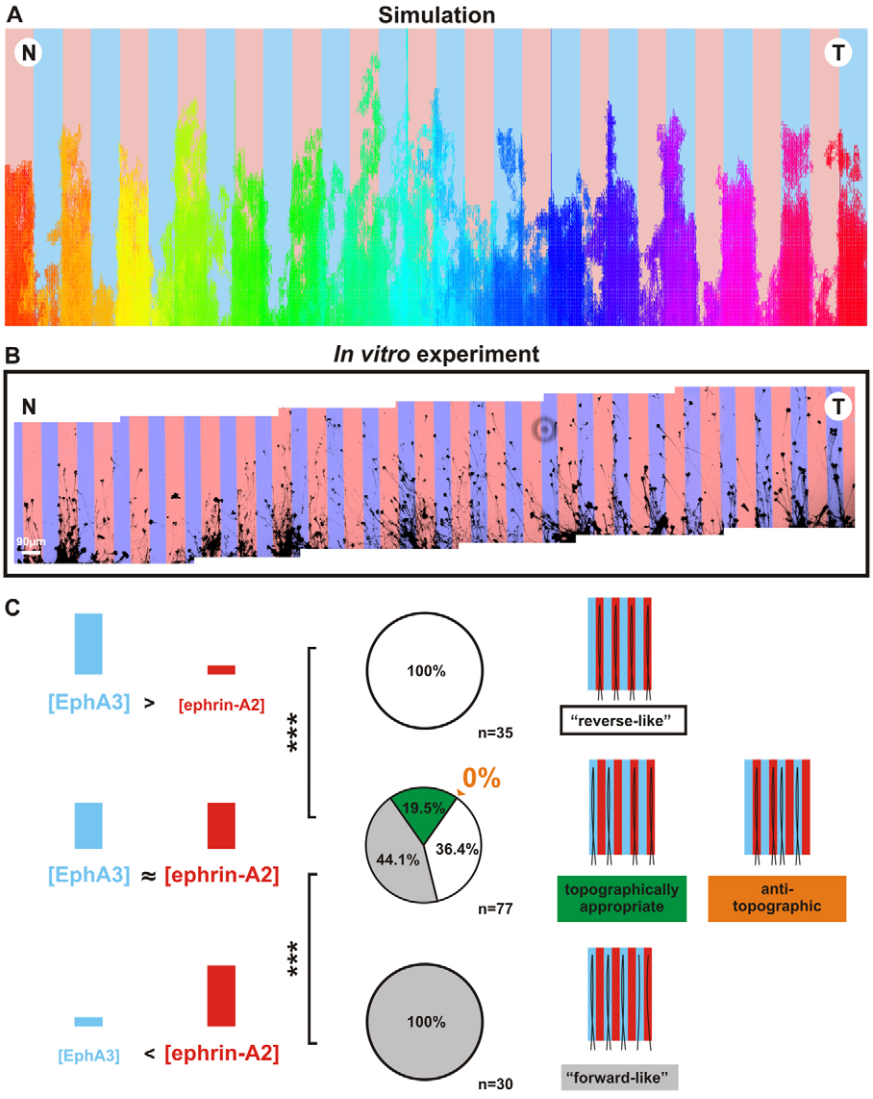

Fig. 6. Topographically appropriate decision of retinal fibers on substrates with alternating receptor and ligand stripes. (**A**) In simulated double-cue stripe assays, nasal fibers grow on the ligand (red: L_{T1}=1, R_{T1}=0, resembling posterior tectum) and temporals on the receptor (blue: L_{T2}=0, R_{T2}=1, resembling anterior tectum) [*n*=300, 3000 iterations, 600×100 field, 30 stripes each (20×100)]. (**B**) Consistent with the simulation, temporal and nasal fibers showed topographically appropriate substrate choice on alternating stripes of ephrin-A2 (red) and EphA3 (blue). (**C**) Quantification of in vitro experiments: at high EphA3 (50 μg/ml) versus low ephrin-A2 (8 μg/ml; first row), retinal fibers always avoided EphA3 stripes ('reverse-like'). Using low EphA3 (20 μg/ml) versus high ephrin-A2 (20 μg/ml) activity (third row), fibers always avoided ephrin-A2 stripes ('forward-like'). At intermediate concentrations (second row, 30 μg/ml EphA3, 16 μg/ml ephrin-A2), a topographically appropriate substrate choice occurs in 19.5% of cases (P<0.005, k*2-chi-square test after Brandt-Snedecor). An anti-topographic decision (nasals on EphA3, temporals on ephrin-A2) was never observed.

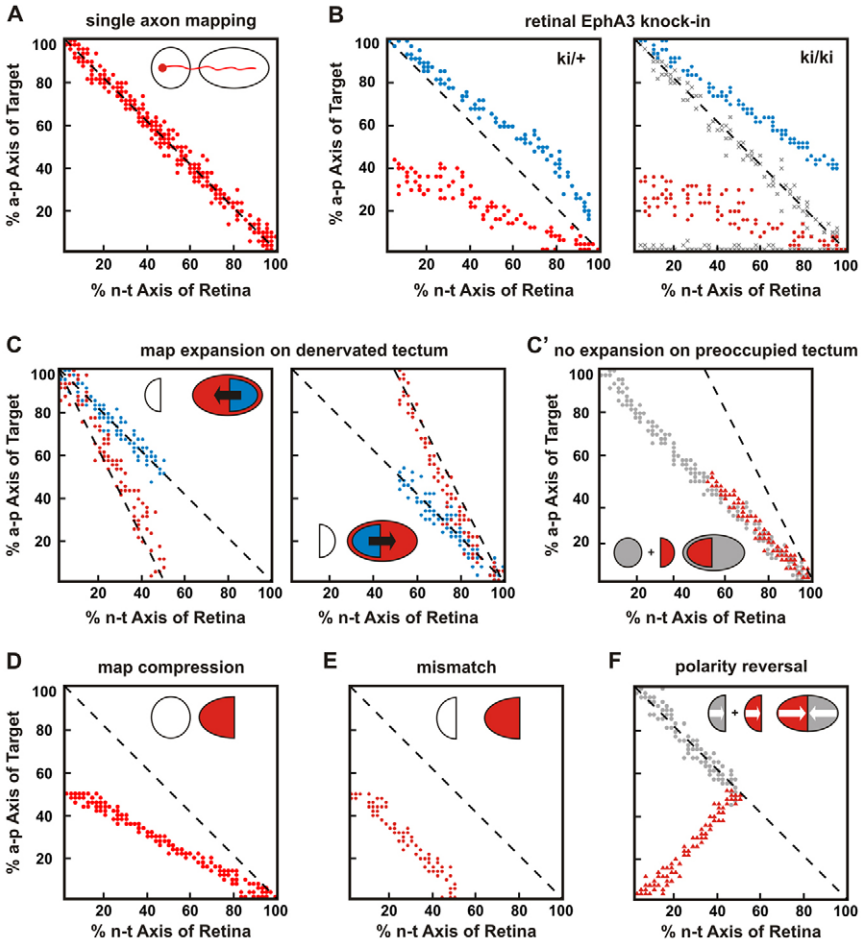

Fig. 7. Modeling in vivo evidence for rigid and adaptive mapping. (**A**) Three-hundred simulations of single fibers chosen randomly from the retinal field. Consistent with the experimental evidence in zebrafish, single fibers map topographically, as indicated by the accumulation of terminals on the main diagonal of the mapping plot. (**B**) EphA3 knock-in, R_{ki}, in every second fiber (red; ki/+→R_{ki}=2; ki/ki→R_{ki}=4; axonal ligand on knock-in fibers was reduced reciprocally to the axonal receptor). Consistent with the experiment, wild-type fibers (blue) were posteriorly displaced, with a more severe effect in homozygotes. Without FF interactions (C_0=0) no displacement is observed (gray crosses). (**C**) Map expansion. One-hundred fibers randomly chosen from the nasal or temporal half of the retina reached their correct target (blue) after 5000 iterations. After 30,000 iterations, fibers stably covered the whole tectum (red). (**C′**) No expansion occurred (red) when temporals grew into a field containing the remnants of a previous innervation (gray). (**D**) Map compression. Two-hundred fibers from a whole retina formed a compressed topographic projection (red) when growing into a 25×8 field representing the anterior tectum. (**E**) Mismatch. 100 nasal fibers formed a half-projection (red), when growing into a 25×8 field representing the anterior, non-matching tectal half. (**F**) An additional nasal projection (red) displayed polarity reversal when growing into a tectal field still containing properly mapped nasal fibers (gray) [*n*=100; FF interactions were put into effect earlier than usual, i.e. k=100 in C(i), see Materials and methods].

To simulate compression (Gaze and Sharma, 1970), we placed 200 terminals randomly chosen from the full retina on a field representing the anterior half-tectum. Consistent with the experimental observation, the model reproduces a stable compressed map on the anterior tectal half (Fig. 7D).

Mismatch experiments (Horder, 1971) were simulated by placing 100 random terminals from the nasal half-retina on a field representing an anterior half-tectum. In accordance with the in vivo evidence, a normally oriented half-map is formed on the foreign target (Fig. 7E).

For the simulation of polarity reversal experiments (Meyer, 1979), the first 100 n-terminals were allowed to invade the p-tectum. They were treated as fixed fiber-derived cues when we subsequently added another 100 randomly chosen n-terminals to the field. Now, the additional nasal innervation formed a reversed map covering the anterior half-tectum, as in the corresponding experiments (Fig. 7F). In this case, the anterior border of the original nasal population forms an anchoring point for the unfolding of a FF chemospecificity-driven map.

DISCUSSION

In separation, reverse and forward ephrin-A/EphA signaling merely evoke graded repulsion in the growth cones of RGCs, instead of providing topographically appropriate guidance. Using novel double-cue (receptor/ligand) stripe substrates, we show that proper topographic guidance, driven by FT chemospecificity, emerges in the simultaneous presence of both cues. The peculiar molecular mechanism based on bidirectional signaling entails FF interactions. We propose those to be central to a concurrent targeting mechanism, driven by FF chemospecificity, which eventually even prevails once terminal arborizations start to develop. Such an extended chemospecificity model in computational simulations accounts for the rigidity of topographic mapping, but also for its highly adaptive features, which pose notorious problems to models based on pure FT chemospecificity. Axon targeting in our model simply amounts to the navigating terminals seeking balance of reverse and forward signaling.

The results of our single-cue stripe assays using ephrin-A2 and EphA3, both prominently expressed in the chick tectum (Cheng et al., 1995; Connor et al., 1998), confirm previous observations obtained with ephrin-A5 and EphA7 (Drescher et al., 1995; Rashid et al., 2005). Reverse signaling in our hands needs higher cue concentrations than does forward signaling. This might be due to weaker adhesion of the respective recombinant protein to the culture dish. But the action of reverse signaling has typically been more difficult to detect. Thus, in assays using tectal membranes to generate the striped carpet, a membranes never evoked any axonal response, although EphA receptors were most probably contained in these preparations (Walter et al., 1987). Reverse signaling might generally be weakened in vitro, possibly owing to a lack of co-factors, such as proBDNF, which is required for efficient signaling via the co-receptor $p75^{NTR}$ (Marler et al., 2010).

A previous study, analyzing outgrowth of explants of varying retinal origin on homogeneous substrates of different ephrin-A2 concentration, concluded that ephrin-A2 would elicit biphasic responses in RGC axons (Hansen et al., 2004). On presumed pre-

target concentrations, axons grew longer than on a neutral substrate. On presumed post-target concentrations, they grew shorter. This is, however, not indicative of a bifunctional mode of action. The biphasic appearance, in this case, is a result of the normalization to growth on the alleged neutral substrate. Actually, the higher the concentration of the cue, the shorter all axons grew, supporting the idea of a monofunctional action.

Our model includes cis-interactions that we suggest will occur whenever the membrane folds back onto itself, e.g. between neighboring filopodia or branchlets of the same terminal. We assume that these interactions simultaneously release reverse and forward signals of equal strengths into the same terminal that are biochemically equivalent to trans-signals. As we have shown, their balancing influence is sufficient to explain the desensitizing effect of cis-interactions in RGCs (Hornberger et al., 1999). Another subtype of cis-interaction is diversely discussed in the literature (Marquardt et al., 2005; Carvalho et al., 2006; Kao and Kania, 2011). It is suggested to occur between directly neighboring ligand and receptor molecules via additional juxtamembrane binding domains and results in masking and signal attenuation. However, recently, this interference has been proposed to occur only when ligands are present in excess relative to the receptor on the same membrane (Kao and Kania, 2011). This might be prevented in chick RGCs by the uniform expression of EphA4, forming a pedestal underneath the EphA3 gradient, which we otherwise omitted for reasons of simplicity.

As predicted by our model, experimental double-cue stripe assays, to our knowledge for the first time under molecularly defined in vitro conditions, yield topographically appropriate guidance choices of RGC growth cones. This remarkable result is seen in about 20% of the experiments. It is validated by two inherent controls. First, n-fibers switch onto the ligand stripe in double-cue when compared with the ligand single-cue assays, whereas temporals on the same substrate continue to avoid the ligand stripes, proving their functionality. The same is true for the temporal subpopulation and receptor stripes. Second, no single explant was found where n-axons grew on EphA and t-axons on the ephrin-A, which would amount to ‘anti-topographic’ behavior. This indicates that the occurrence of topographically appropriate guidance is highly significant and failures are due to experimental fluctuations. There is a singular previous report of topographically correct RGC fiber growth in vitro (von Boxberg et al., 1993). For their stripe assays, the authors used tectal membranes purified by a special fractionation technique. Like us, they observed topographically appropriate choices in a minority of cases. As brain membranes are poorly defined substrates, the molecular underpinnings of those results have remained elusive. Conceivably, the special technique for the preparation of tectal membranes may have resulted in the enrichment of receptor activity in a-membranes.

Central to our model is the idea of FF chemospecificity based on mutual topographically appropriate repulsion. We assume these interactions to be conveyed by growth cones initially and later predominantly by growing terminal arborizations. When RGC axons are given the choice to grow on nasal or temporal retinal axons, nasals show no preference, but temporals exclusively choose t-axons (Bonhoeffer and Huf, 1985). This selectivity is based on repulsion, because temporal growth cones retract on contact with n-axons (Raper and Grunewald, 1990). The lack of responsiveness of nasal growth cones in these experiments might again be due to disproportionate weakness of reverse signaling in vitro. It remains to be investigated, whether these interactions are based on the ephrin-A/EphA system, as we propose. The fact that in EphA3 knock-in mice (Brown et al., 2000), EphA3 overexpressing axons displace wild-type axons is, however, consistent with the suggested model.

Numerous computational models have attempted to simulate topographic mapping (reviewed by Goodhill and Xu, 2005). We adopt the mechanism of terminal movement from the servomechanism model (Honda, 1998), which differs strongly, however, by relying purely on bifunctional ephrin-A forward signaling. The competition/servomechanism model (Honda, 2003) additionally incorporates competitive FF interactions that depend on FT interactions hampering the ability of the model to fully replicate adaptive mapping. Yates et al. (Yates et al., 2004), like us, implement bidirectional ephrin-A/EphA signaling for FT and FF interactions. In stark contrast, however, axon targeting in their model relies on interstitial branching instead of primary growth cone guidance. Simulations, therefore, start out with the main axons pre-positioned and fixed on the target field. Thus, the impact of FF interactions is strongly locally confined, severely limiting their potential to account for adaptive mapping. At least four models comprehensively addressed the evidence for rigid and adaptive mapping. All of them agree with our model on the necessity of FT and independent FF interactions that eventually exceed FT interactions. Two of them, however, do not address any actual axon growth process. The multiple-constraints model (Fraser and Perkel, 1990) considers minimization of ensemble free energies via simulated annealing, whereas the model by Weber et al. (Weber et al., 1997) simulates the temporal dynamics of a synaptic weight matrix using differential equations. Though invaluable in proving that rigid and adaptive topographic mapping could be reconciled in one model, they are not easily related to experimentally derived molecular and cellular mechanisms. The retinal induction model, by contrast, proposes a distinct mechanism (Willshaw, 2006). On innervation, terminals are supposed to induce ephrins spreading locally in the naïve target. Inductive potency is iteratively readjusted, proportionate to the marker matching between terminal and target resulting in topographic sorting by cooperation of topographically similar and competition of dissimilar terminals. To date, however, experimental evidence for the proposed induction is lacking. Imported axonal ephrin-A might fulfill comparable roles in our model. A recent update (Simpson and Goodhill, 2011) of the extended branch arrow model (Overton and Arbib, 1982) uses EphA receptor activities for ratiometric comparisons of axons in FF interactions, but not for FT chemospecificity. The model thus cannot account for any in vitro stripe assay results.

It might be speculated that signaling interactions resembling those proposed here could represent evolutionary adaptations for an axonal mapping that is concomitantly topographically precise and robust.

Long-range projections connect neuronal layers, which are distant and, therefore, unlikely to match precisely in size and expression of guidance markers, as required by pure FT chemospecificity. The conceivably most robust mechanism to map projecting axons onto such target fields is to use FF chemospecificity, i.e. to bring in the sorting apparatus with the terminals and to assure that they will spread to cover the whole field. This poses special constraints on the signaling system.

First, in a FF interaction model primary signal strength not only depends on topographic identity but also on the variable spacing of the interacting terminals. The use of two monofunctional guidance cues (in contrast to one bifunctional cue) provides an effective way

to disambiguate signal strength. This is because the ratio of the two signals, which can be used to encode topographic identity, is independent of the spacing of the interacting terminals.

Second, the simultaneous presence of guidance signals and cognate receptors on the same terminal, inherent to any FF interaction model, necessitates cis-interactions, posing a problem of self/non-self discrimination. Bidirectional signaling provides a highly parsimonious solution to this problem. If forward and reverse signals are implemented to balance each other, every imbalance will signify an external signal source. The only exception is a signal source that exactly matches the receptor/ligand endowment of the sensing terminal and corresponds to its sought target.

The signaling system described so far would be sufficient for topographic sorting. Relying completely on FF chemospecificity, however, requires large numbers of comparisons to be made among the self-sorting terminals. This will probably be inefficient, if it is to be based on slowly moving axon terminals. FT chemospecificity might therefore, in addition to providing global map orientation, be used as an auxiliary presorting mechanism, so that ineffective comparisons of topographically disparate terminals are suppressed, while productive comparisons of closer neighbors are enforced.

Once enough terminals have invaded the target and start growing, a smooth transition from FT to FF chemospecificity-based targeting will take place. As terminals cannot distinguish the actual source of an impinging signal, the only constraint governing their target approach in this model is the tendency to balance forward and reverse signaling. Given the amazing simplicity of this mechanism, the widespread occurrence of topographic projections might be due more to the ease of their development, than to any functional advantage.

Acknowledgements
We thank Anne von Philipsborn for ideas on fabricating double-cue stripe carpets, Jett Thor van Note for help with language editing and Friedrich Bonhoeffer for helpful comments on the manuscript.

Funding
This work was supported by the German Research Foundation (DFG) [KSOP-grant GSC21/1 to C.G., grant BA1034/14-3 to M.B. and F.W.]; and the Federal Ministry of Education and Research (BMBF) [grant 01ZZ0405 to F.W.].

Competing interests statement
The authors declare no competing financial interests.

Supplementary material
Supplementary material available online at
http://dev.biologists.org/lookup/suppl/doi:10.1242/dev.070474/-/DC1

References

Attardi, D. G. and Sperry, R. W. (1963). Preferential selection of central pathways by regenerating optic fibers. *Exp. Neurol.* **7**, 46-64.
Bonhoeffer, F. and Huf, J. (1982). In vitro experiments on axon guidance demonstrating an anterior-posterior gradient on the tectum. *EMBO J.* **1**, 427-431.
Bonhoeffer, F. and Huf, J. (1985). Position-dependent properties of retinal axons and their growth cones. *Nature* **315**, 409-410.
Brown, A., Yates, P. A., Burrola, P., Ortuno, D., Vaidya, A., Jessell, T. M., Pfaff, S. L., O'Leary, D. D. and Lemke, G. (2000). Topographic mapping from the retina to the midbrain is controlled by relative but not absolute levels of EphA receptor signaling. *Cell* **102**, 77-88.
Carvalho, R. F., Beutler, M., Marler, K. J., Knoll, B., Becker-Barroso, E., Heintzmann, R., Ng, T. and Drescher, U. (2006). Silencing of EphA3 through a cis interaction with ephrinA5. *Nat. Neurosci.* **9**, 322-330.
Cheng, H. J., Nakamoto, M., Bergemann, A. D. and Flanagan, J. G. (1995). Complementary gradients in expression and binding of ELF-1 and Mek4 in development of the topographic retinotectal projection map. *Cell* **82**, 371-381.
Connor, R. J., Menzel, P. and Pasquale, E. B. (1998). Expression and tyrosine phosphorylation of Eph receptors suggest multiple mechanisms in patterning of the visual system. *Dev. Biol.* **193**, 21-35.
Drescher, U., Kremoser, C., Handwerker, C., Loschinger, J., Noda, M. and Bonhoeffer, F. (1995). In vitro guidance of retinal ganglion cell axons by RAGS, a 25 kDa tectal protein related to ligands for Eph receptor tyrosine kinases. *Cell* **82**, 359-370.
Feldheim, D. A. and O'Leary, D. D. (2010). Visual map development: bidirectional signaling, bifunctional guidance molecules, and competition. *Cold Spring Harb. Perspect. Biol.* **2**, a001768.
Feldheim, D. A., Kim, Y. I., Bergemann, A. D., Frisen, J., Barbacid, M. and Flanagan, J. G. (2000). Genetic analysis of ephrin-A2 and ephrin-A5 shows their requirement in multiple aspects of retinocollicular mapping. *Neuron* **25**, 563-574.
Feldheim, D. A., Nakamoto, M., Osterfield, M., Gale, N. W., DeChiara, T. M., Rohatgi, R., Yancopoulos, G. D. and Flanagan, J. G. (2004). Loss-of-function analysis of EphA receptors in retinotectal mapping. *J. Neurosci.* **24**, 2542-2550.
Fraser, S. E. and Perkel, D. H. (1990). Competitive and positional cues in the patterning of nerve connections. *J. Neurobiol.* **21**, 51-72.
Gaze, R. M. and Sharma, S. C. (1970). Axial differences in the reinnervation of the goldfish optic tectum by regenerating optic nerve fibres. *Exp. Brain Res.* **10**, 171-181.
Gierer, A. (1981). Development of projections between areas of the nervous system. *Biol. Cybern.* **42**, 69-78.
Goodhill, G. J. and Richards, L. J. (1999). Retinotectal maps: molecules, models and misplaced data. *Trends Neurosci.* **22**, 529-534.
Goodhill, G. J. and Xu, J. (2005). The development of retinotectal maps: a review of models based on molecular gradients. *Network* **16**, 5-34.
Gosse, N. J., Nevin, L. M. and Baier, H. (2008). Retinotopic order in the absence of axon competition. *Nature* **452**, 892-895.
Hansen, M. J., Dallal, G. E. and Flanagan, J. G. (2004). Retinal axon response to ephrin-As shows a graded, concentration-dependent transition from growth promotion to inhibition. *Neuron* **42**, 717-730.
Honda, H. (1998). Topographic mapping in the retinotectal projection by means of complementary ligand and receptor gradients: a computer simulation study. *J. Theor. Biol.* **192**, 235-246.
Honda, H. (2003). Competition between retinal ganglion axons for targets under the servomechanism model explains abnormal retinocollicular projection of Eph receptor-overexpressing or ephrin-lacking mice. *J. Neurosci.* **23**, 10368-10377.
Horder, T. J. (1971). Retention, by fish optic nerve fibres regenerating to new terminal sites in the tectum, of 'chemospecific' affinity for their original sites. *J. Physiol.* **216**, 53P-55P.
Hornberger, M. R., Dutting, D., Ciossek, T., Yamada, T., Handwerker, C., Lang, S., Weth, F., Huf, J., Wessel, R., Logan, C. et al. (1999). Modulation of EphA receptor function by coexpressed ephrinA ligands on retinal ganglion cell axons. *Neuron* **22**, 731-742.
Kao, T. J. and Kania, A. (2011). Ephrin-mediated cis-attenuation of Eph receptor signaling is essential for spinal motor axon guidance. *Neuron* **71**, 76-91.
Lemke, G. and Reber, M. (2005). Retinotectal mapping: new insights from molecular genetics. *Annu. Rev. Cell Dev. Biol.* **21**, 551-580.
Luo, L. and Flanagan, J. G. (2007). Development of continuous and discrete neural maps. *Neuron* **56**, 284-300.
Marler, K. J., Poopalasundaram, S., Broom, E. R., Wentzel, C. and Drescher, U. (2010). Pro-neurotrophins secreted from retinal ganglion cell axons are necessary for ephrinA-p75NTR-mediated axon guidance. *Neural Dev.* **5**, 30.
Marquardt, T., Shirasaki, R., Ghosh, S., Andrews, S. E., Carter, N., Hunter, T. and Pfaff, S. L. (2005). Coexpressed EphA receptors and ephrin-A ligands mediate opposing actions on growth cone navigation from distinct membrane domains. *Cell* **121**, 127-139.
McLaughlin, T., Torborg, C. L., Feller, M. B. and O'Leary, D. D. (2003). Retinotopic map refinement requires spontaneous retinal waves during a brief critical period of development. *Neuron* **40**, 1147-1160.
Meyer, R. L. (1979). Retinotectal projection in goldfish to an inappropriate region with a reversal in polarity. *Science* **205**, 819-820.
Monschau, B., Kremoser, C., Ohta, K., Tanaka, H., Kaneko, T., Yamada, T., Handwerker, C., Hornberger, M. R., Loschinger, J., Pasquale, E. B. et al. (1997). Shared and distinct functions of RAGS and ELF-1 in guiding retinal axons. *EMBO J.* **16**, 1258-1267.
Overton, K. J. and Arbib, M. A. (1982). The extended branch-arrow model of the formation of retino-tectal connections. *Biol. Cybern.* **45**, 157-175.
Raper, J. A. and Grunewald, E. B. (1990). Temporal retinal growth cones collapse on contact with nasal retinal axons. *Exp. Neurol.* **109**, 70-74.
Rashid, T., Upton, A. L., Blentic, A., Ciossek, T., Knoll, B., Thompson, I. D. and Drescher, U. (2005). Opposing gradients of ephrin-As and EphA7 in the superior colliculus are essential for topographic mapping in the mammalian visual system. *Neuron* **47**, 57-69.
Reber, M., Burrola, P. and Lemke, G. (2004). A relative signalling model for the formation of a topographic neural map. *Nature* **431**, 847-853.
Schmidt, J. T., Cicerone, C. M. and Easter, S. S. (1978). Expansion of the half retinal projection to the tectum in goldfish: an electrophysiological and anatomical study. *J. Comp. Neurol.* **177**, 257-277.
Simpson, H. D. and Goodhill, G. J. (2011). A simple model can unify a broad range of phenomena in retinotectal map development. *Biol. Cybern.* **104**, 9-29.

Sperry, R. W. (1963). Chemoaffinity in the orderly growth of nerve fiber patterns and connections. *Proc. Natl. Acad. Sci. USA* **50**, 703-710.
Tsigankov, D. and Koulakov, A. A. (2010). Sperry versus Hebb: topographic mapping in Isl2/EphA3 mutant mice. *BMC Neurosci.* **11**, 155.
van Ooyen, A. (2011). Using theoretical models to analyse neural development. *Nat. Rev. Neurosci.* **12**, 311-326.
Vielmetter, J., Stolze, B., Bonhoeffer, F. and Stuermer, C. A. (1990). In vitro assay to test differential substrate affinities of growing axons and migratory cells. *Exp. Brain Res.* **81**, 283-287.
von Boxberg, Y., Deiss, S. and Schwarz, U. (1993). Guidance and topographic stabilization of nasal chick retinal axons on target-derived components in vitro. *Neuron* **10**, 345-357.
von Philipsborn, A. C., Lang, S., Bernard, A., Loeschinger, J., David, C., Lehnert, D., Bastmeyer, M. and Bonhoeffer, F. (2006). Microcontact printing of axon guidance molecules for generation of graded patterns. *Nat. Protoc.* **1**, 1322-1328.
von Philipsborn, A. C., Lang, S., Jiang, Z., Bonhoeffer, F. and Bastmeyer, M. (2007). Substrate-bound protein gradients for cell culture fabricated by microfluidic networks and microcontact printing. *Sci. STKE* **2007**, pl6.
Walter, J., Kern-Veits, B., Huf, J., Stolze, B. and Bonhoeffer, F. (1987). Recognition of position-specific properties of tectal cell membranes by retinal axons in vitro. *Development* **101**, 685-696.
Weber, C., Ritter, H., Cowan, J. and Obermayer, K. (1997). Development and regeneration of the retinotectal map in goldfish: a computational study. *Philos. Trans. R. Soc. Lond. B Biol. Sci.* **352**, 1603-1623.
Willshaw, D. (2006). Analysis of mouse EphA knockins and knockouts suggests that retinal axons programme target cells to form ordered retinotopic maps. *Development* **133**, 2705-2717.
Yates, P. A., Holub, A. D., McLaughlin, T., Sejnowski, T. J. and O'Leary, D. D. (2004). Computational modeling of retinotopic map development to define contributions of EphA-ephrinA gradients, axon-axon interactions, and patterned activity. *J. Neurobiol.* **59**, 95-113.